Covalent double functionalization of graphene oxide for proton conductive and redox-active functions

Rizwan Khan, Keita Miyagawa, Alberto Bianco, Yuta Nishina

Covalent double functionalization of graphene oxide for proton conductive and redox-active functions

Rizwan Khan,[a,b] Keita Miyagawa,[a] Alberto Bianco,[c] Yuta Nishina[*a,b]

[a]*Graduate School of Natural Science and Technology, Okayama University, 3-1-1 Tsushima-naka, kita-ku, Okayama, 700-8530, Japan.*
[b]*Research Core for Interdisciplinary Sciences, Okayama University, 3-1-1 Tsushima-naka, kita-ku, Okayama, 700-8530, Japan.*
[c]*CNRS, Immunology, Immunopathology and Therapeutic Chemistry, UPR3572, University of Strasbourg, ISIS, Strasbourg, 67000, France*
E-mail: nisina-y@cc.okayama-u.ac.jp

Keywords : Carbon materials, graphene, multi-functionalization, proton conductivity, energy storage

Abstract

The covalent double functionalization of graphene oxide (GO) is an effective approach to tune the properties of graphene-like materials. The first step is the ring-opening reaction of epoxides by amines, followed by the second step consisting on the nucleophilic addition reaction of GO hydroxyl groups to an α,β-unsaturated carbonyl compound. The benefit of doubly functionalized GO is to possess different functions, confirmed by measuring proton conductivity and supercapacitor performance. The proton conductivity can be improved by introducing sulfonic acid and redox-active functional groups on GO, while the capacitance for supercapacitor can be increased by introducing two distinct redox-active molecules. The current study evidences that a double functionalization allow to design a multifunctional GO platform as an electrolyte membrane for fuel cells and/or an electrode material for supercapacitors.

1. Introduction

GO and its derivatives have attracted considerable interest from academics and because they can be synthesized on a large scale with reasonable cost, and their functions can be improved by chemical treatment through modification of their oxygenated functional groups [1,2]. The applications of functionalized GO have been actively investigated for the development of new types of transistors [3], transparent electrodes [4], sensors [5-7], polymer composites [8-10], ultrastrong materials [11], electrocatalysts [12-14], and energy storage devices [15,16]. Covalent derivatization of GO sometimes causes simultaneous reduction GO while preventing stacking of GO layers [17]. Esterification of the carboxylic acids [18], reaction of the carboxy and hydroxy groups with isocyanate derivatives [19], Williamson reaction [20], silanization of the hydroxy groups [21], Claisen rearrangement [22], and ring opening reaction of epoxides [23] have been developed for GO functionalization. GO have a limited amount of carboxyl groups at the edges, which may lead to low level of functionalization. In contrast, basal plane functionalization is more desirable to introduce as many functions as possible. In this context, nucleophilic addition to epoxide [24], and functionalization of hydroxyl groups [25], have been widely investigated.

Besides monofunctionalization of GO described above, covalent double functionalization allows the attachment of additional target molecules stepwisely. Only a few strategies for the covalent double functionalization of GO have been reported so far. Some studies developed the combination of epoxide ring opening and Steglich esterification of carboxyl group [26], or the combination of epoxide ring opening and Michael addition [25, 27]. The previous studies evidenced that the double functionalization of GO can introduce various functional groups, but targeted applications have not been explored in detail. In this work, we focused our attention on the covalent double functionalization of GO to tune its electrochemical properties and applied for the preparation of advanced electrode materials. To this end, two different organic molecules with specific functions were introduced onto GO using a stepwise covalent double functionalization. The first step consisted of the ring-opening reaction of epoxide groups of GO with amino compounds, while the second step involved the nucleophilic addition of hydroxyl groups on GO to an α,β-unsaturated carbonyl compound. The advantage of this strategy was confirmed by measuring proton conductivity and capacitance for supercapacitor. The proton conductivity was improved by introducing sulfonic acid and redox-active functional groups onto

GO, while the capacitance for supercapacitor was increased by introducing more redox-active molecules.

2. Experimental section

2.1. Chemicals and materials

Natural graphite flakes (99.8%) were obtained from Alfa Aesar. 1,4-Benzoquinone, methyl vinylketone, propylamine and aniline weres obtained from Tokyo chemical industry Co., Ltd. Toluene was obtained from Kanto chemical co. inc. Potassium permanganate ($KMnO_4$), sulfuric acid (H_2SO_4, 96%), ethanol, sodium azide, acetic acid, tetrahydrofuran, 1,4-naphthoquinone and sulfanilic acid were obtained from Wako Co., Ltd. All reagents and solvent were used as received.

2.2. Synthesis of 2-amino-1,4-naphthoquinone

The synthesis was performed following the reported method [28]. A round-bottom flask equipped with a magnetic stir bar was charged with 1,4-naphthoquinone (2.37 g, 15 mmol, 1.0 equiv.) and H_2O/THF (1:4, 50 mL). To this solution, a solution of sodium azide (2.93 g, 45 mmol, 3.0 equiv.) and acetic acid (3 mL) in distilled water (8 mL) was added and stirred at room temperature. After 7 h, the reaction was concentrated in vacuo and the residue was dissolved in ethyl acetate. The resulting solution was washed with 1 M NaOH, extracted with ethyl acetate, and washed with saturated NaCl. The organic layer was dried over $MgSO_4$ and the solvent was removed in vacuo. The crude residue was purified by silica gel column chromatography (hexane/ethyl acetate = 1/2) to give 2.3 g (89%) as a brown solid. ^{1}H-NMR (400 MHz, $CDCl_3$): δ 7.94 (dd, J = 7.15, 19.70 Hz, 2H), 7.82 (dt, J = 1.00, 7.53 Hz, 1H), 7.69 - 7.76 (m, 1H), 5.82 (s, 1H).

2.3. Synthesis of graphene oxide (GO)

Graphite powder (100 g) was dispersed into concentrated H_2SO_4 (2.5 L). After cooling the mixture in an ice bath, $KMnO_4$ (300 g) was added, and the reaction mixture was kept below 55 °C. The mixture was stirred at 35 °C for 2 h to complete the oxidation process. Next, deionized water (5 L) was slowly added, and the temperature was kept below 50 °C with continuous stirring, then H_2O_2 (30% aq., 250 mL) was added into the mixture. Finally, the brown

crude graphite oxide was purified by performing 10 times centrifugation, affording GO. Concentration of GO was measured by drying the GO dispersion under vacuum at 50 °C. The size of obtained GO was 2 μm [29].

*2.4. General procedure for the synthesis of **GO 1** and **GO 5***

In a typical procedure, aniline or propylamine (1 mL) was added dropwise to the suspension of GO in water (250 mg L^{-1}, 400 mL) under vigorous stirring. The GO The resulting mixture was stirred for additional 24 h at room temperature, then filtered and thoroughly washed with ethanol and water several times. The obtained solid was freeze-dried for two days.

*2.5. General procedure for the synthesis of **GO 2a-c**, **GO 4**, **GO 6**, **GO 7**, and **GO 9***

To a dispersion of GO (40 mg) in toluene (5 mL), a solution of the α,β-unsaturated carbonyl compounds (300 mg) in toluene (10 mL) was added. The mixture was refluxed for 36 h at 112 °C with constant stirring. After completion of reaction, the mixture was filtered and washed with water and toluene several times, respectively. The sample was then dried under vacuum for two days at 50 °C.

*2.6. Synthesis of **GO 3** and **GO 8***

In a typical procedure, the compound with the primary amine function (300 mg) was dissolved in 30 mL ethanol and then added to GO aqueous dispersion (10 mL, 10 mg mL^{-1}, 100 mg). The mixture was sonicated for 1 h to get a homogeneous dispersion. The dispersion was refluxed for 48 h and purified by centrifugation and washing (ethanol and then water, 3 times each). The product was finally freeze-dried for two days.

2.7. Instruments and measurements

The functional groups on the surface of GO were analyzed using a Fourier transform infrared spectrometer (FT-IR, SHIMADZU, IR Tracer 100), (KBr pellet). The elemental compositions were determined by X-ray photoelectron spectroscopy (XPS). The XPS was carried out on a JPS-9030 with a pass energy of 20 eV.

The electrochemical behavior of prepared samples was measured using three electrode system. In the three-electrode system, the platinum foil and Ag/AgCl electrode were used as the counter

electrode and reference electrode, respectively. The working electrode was fabricated by mixing electrode material (4 mg) and carbon black (0.7 mg) in 0.4 mL Nafion solution, which is sonicated for 1 h to make fine dispersion. Then, 3 μL of the above suspension were dropped using a pipet gun onto the glassy carbon electrode (3 mm) and completely dried at 50 °C for 1 h under vacuum. The electrochemical performance was measured in a potential range of -0.6-0.8 V, with a scan rate of 50 mVs^{-1}. All electrochemical experiments were performed in 0.5 M H_2SO_4 aqueous electrolyte. The specific capacitance (C ($F\ g^{-1}$)) of the supercapacitor was calculated from the discharge curve according to the following formula:

$$C = (I \times \Delta t)/(m \times \Delta V)$$

where I is the constant current in discharging, m is the mass of active material on the working electrode, Δt is the discharge time, and ΔV is the voltage change during discharge.

For proton conductivity, the sample was pressed into 10 mm diameter pellets. The thickness of the pellet for **GO 4** and **GO 6** was 0.414 mm 0.25 mm, respectively. The sample electrode was sandwiched between the two stainless steel spacers and assembled [30]. The electrochemical impedance test was conducted at a frequency range of 1000 kHz to 1 Hz at 0 V with an AC perturbation of 10 mV. The proton conductivity was measured by following by equation:

$$\sigma = (L)/(Z .A)$$

where σ is the proton conductivity, L is the thickness of the electrode, Z is impedance value and A is the electrode surface area.

3. Results and Discussion

3.1. Functionalization of GO

Initially, GO (Fig. S1) was functionalized by simple organic molecules to optimize the double functionalization conditions. The first step consisted of the reaction of propylamine with the epoxide groups of GO [31-33], allowing to introduce the first functionality and to generate more hydroxyl groups (Fig. 1a), which subsequently reacted with α,β-unsaturated carbonyl compounds such as methyl vinyl ketone (**a**), 1,4-benzoquinone (**b**) and 1,4-naphthoquinone (**c**) (Fig. 1b) [27].

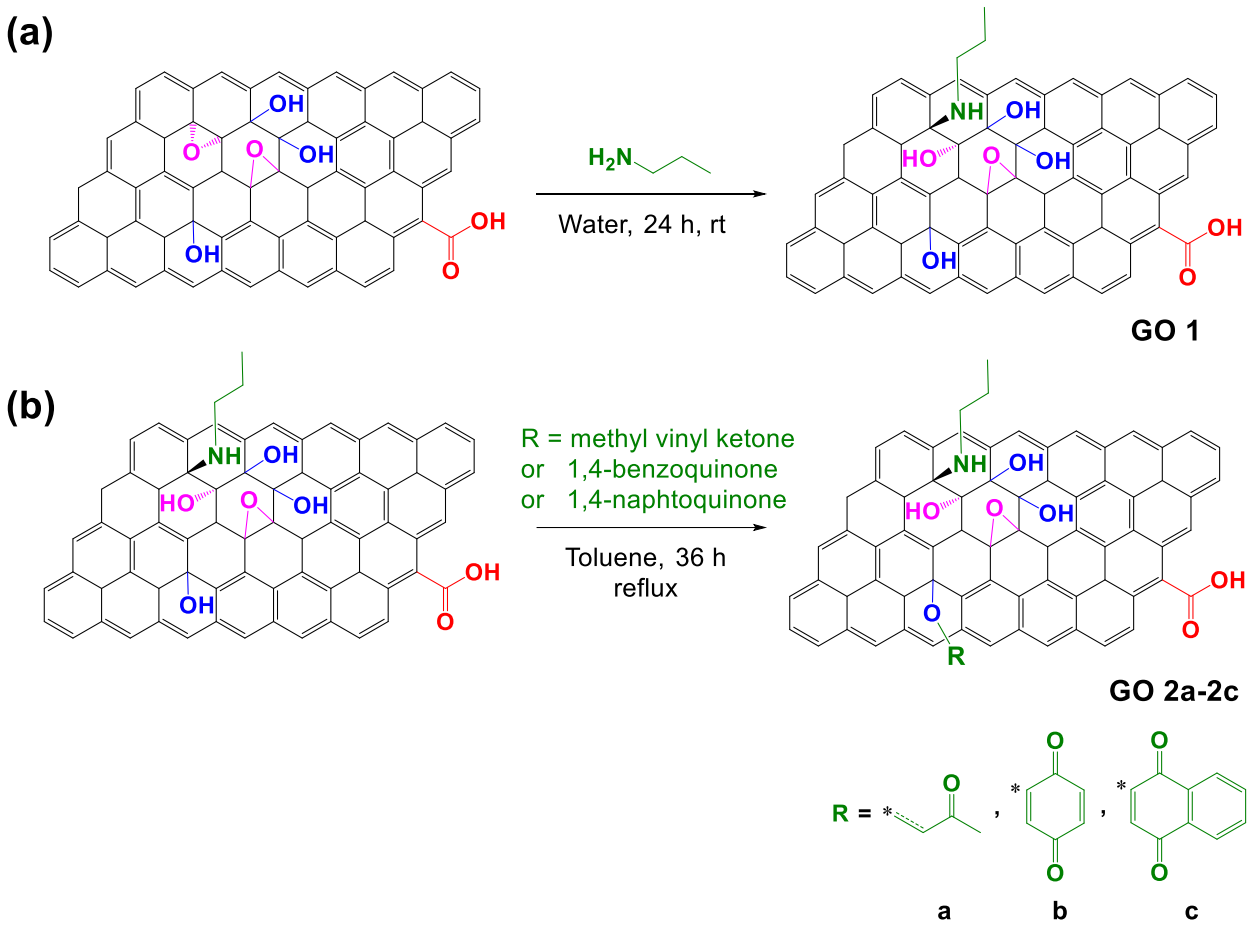

Fig. 1. Synthesis of covalent double functionalized GO. The asterisks indicate the atoms forming the covalent bond with the OH function of GO. The Michael product of methyl vinyl ketone (**GO 2a**) may form C-C or C=C bond, while the products derived from benzoquinone (**GO 2b**) and naphthoquinone (**GO 2c**) are autoxidized to quinone structure, forming C=C bonds. All OH groups can potentially react in the second step. However, only one functionalized OH group is shown for simplicity.

The prepared materials were characterized by X-ray photoelectron spectroscopy (XPS), Fourier-transform infrared spectroscopy (FTIR), and cyclic voltammogram (CV).

The XPS survey analysis showed that propylamine-functionalized GO (**GO 1**) contained carbon, oxygen, and nitrogen (Fig. S2). The amount of oxygen in GO 1 was decreased by functionalization (Table S1), which is indicative of a reduction of GO during amine functionalization, as previously reported [33]. The high-resolution XPS analysis of N 1s peak in **GO 1** appeared at 399.5 eV, attributed to the newly formed N−C bond, thus confirming the amination through epoxide ring-opening reaction (Fig. S3a) [34].

The functionalization of **GO 2a-2c** was also confirmed by the high-resolution C 1s XPS analysis. The XPS spectra of **GO 2a-2c** showed that the peak related to C=O group was increased due to

the introduction of quinone molecules (Fig. 2a (ii-iv)). The percentage of C=O bonds in **GO 1** changed from 4.1% to 5.2%, 6.1%, and 5.9% in **GO 2a**, **GO 2b**, and **GO 2c**, respectively (Fig. 2b) [27,35]. These changes could be explained by the grafting of α,β-unsaturated carbonyl compounds onto GO.

The surface functional groups of GO, **GO 1** and **GO 2a-2c** were further confirmed by FTIR analysis (Fig. 2c). The weak peak at 1250 cm^{-1} was attributed to C-N bond, which confirmed the chemical modification of **GO 1**. As compared to pristine GO, absorbance related to OH bending (at 1380 cm^{-1}) was increased 1.4 times in **GO 1**, confirming the ring opening reaction of epoxide [27]. The absorbance of the OH bending was decreased in **GO 2a-2c**, as compared to **GO 1**, suggesting the consumption of the hydroxyl groups by the second reaction. A peak at 1726 cm^{-1} can be observed in the FTIR spectra of **GO 2a-2c**, assigned to the C=O group, related to the attachment of quinone molecules. A peak at 1726 cm^{-1} can be observed in the FTIR spectra of **GO 2a-2c**, assigned to the C=O group, related to the attachment of quinone molecules. All these changes confirmed the attachment of α,β-unsaturated carbonyl compounds **a**, **b**, and **c** after the epoxide opening (Fig. 2c) [38,39].

To further confirm the double functionalization by Michael addition, CV measurements were performed (Fig. S4). CV is sensitive to the redox-active molecules [40]. The CV curve of **GO 2a** showed no redox peaks, while the CV curve of **GO 2b** and **GO 2c** exhibited the expected redox peaks. The redox peaks for **GO 2b** and **GO 2c** appeared at different potentials [41,42]. The redox potentials of molecules change with a change in the molecular structure [43].

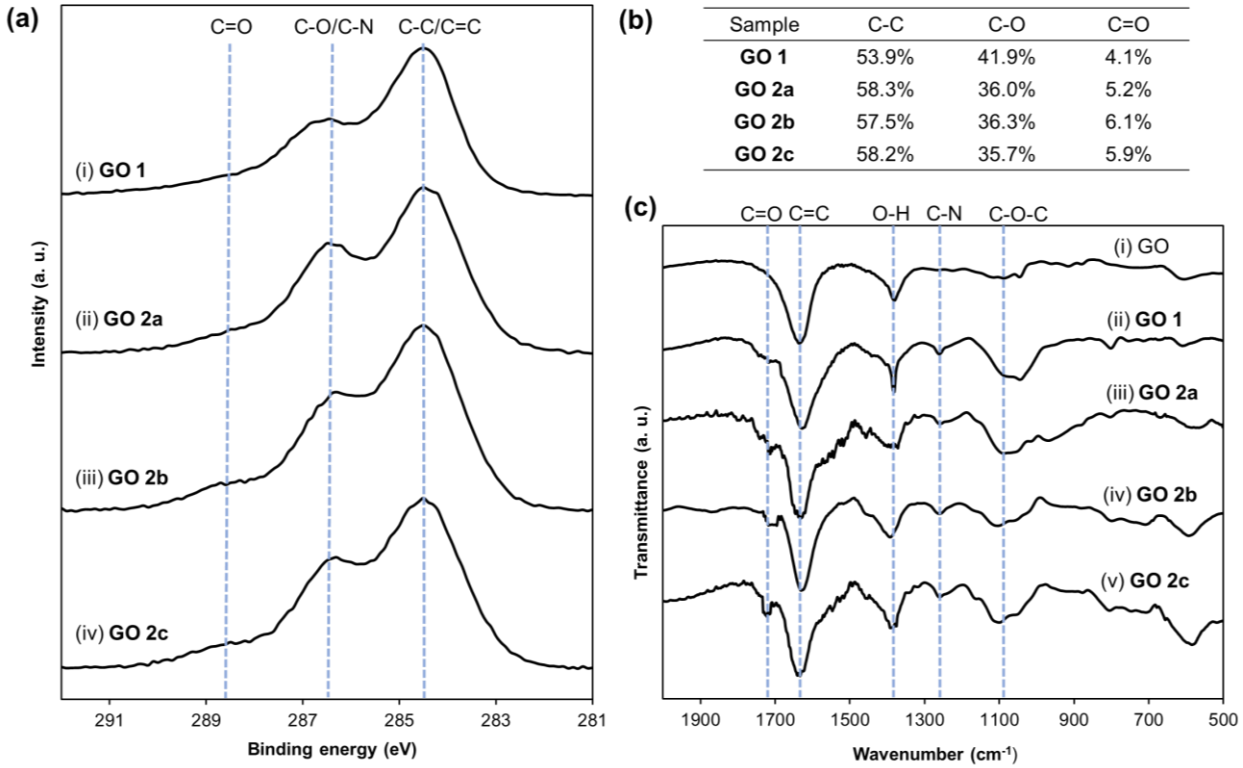

Sample	C-C	C-O	C=O
GO 1	53.9%	41.9%	4.1%
GO 2a	58.3%	36.0%	5.2%
GO 2b	57.5%	36.3%	6.1%
GO 2c	58.2%	35.7%	5.9%

Fig. 2. (a) High-resolution C 1s XPS spectra of (i) **GO 1**, (ii) **GO 2a**, (iii) **GO 2b**, and (iv) **GO 2c** [36,37]; (b) table for the quantitative analysis of high resolution C 1s XPS spectra of **GO 1**, **GO 2a**, **GO 2b**, and **GO 2c**; (c) FTIR spectra of (i) GO, (ii) **GO 1**, (iii) **GO 2a**, (iv) **GO 2b**, and (v) **GO 2c**. The peak associated with C=C bond was used for normalization.

3.2. Double functionalization of GO for improved proton conductivity

To show the usefulness of double functionalized GO, we decided to introduce two different active functions onto GO. GO was first functionalized with sulfanilic acid through epoxide ring-opening reaction leading to conjugate **GO 3**, followed by the addition of benzoquinone (conjugate **GO 4**). In this case, sulfanilic acid acts as a proton conductor [44], and benzoquinone act as redox-active site. For comparison, a non-proton conductive aromatic amine, namely aniline, was covalently linked to GO (conjugate **GO 5**), followed by the addition of benzoquinone (conjugate **GO 6**) (Fig. 3). The prepared materials were analyzed by XPS (see details of the characterization in Section 2 of the Supporting Information).

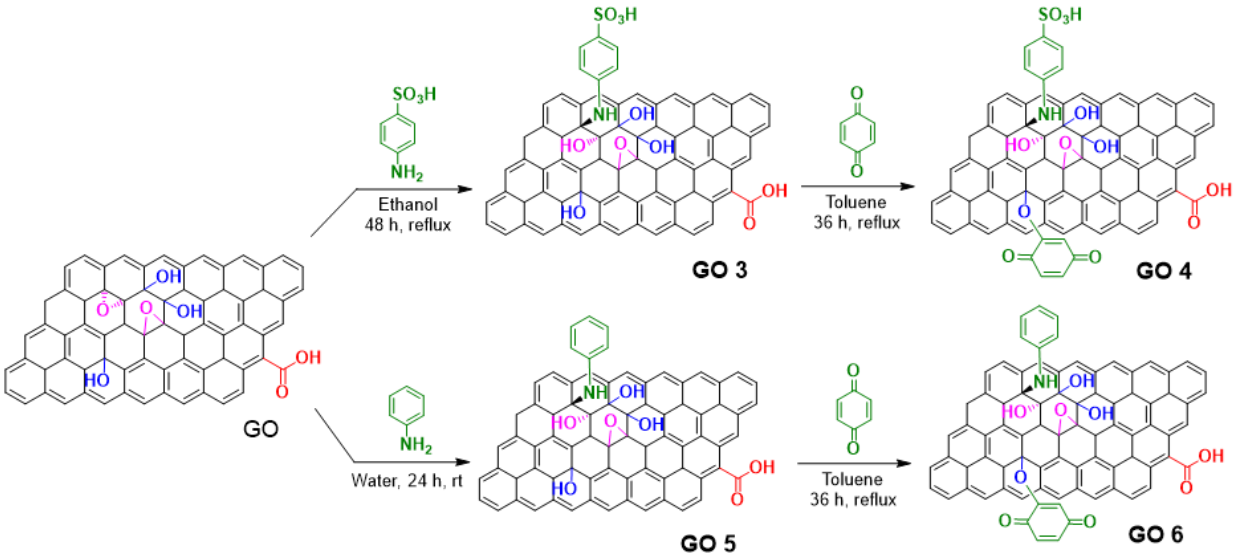

Fig. 3. Synthesis of **GO 3**, **GO 4**, **GO 5**, and **GO 6**. For simplicity, only one epoxide ring is opened in **GO 3** and **GO 5** and one hydroxyl group is derivatized in **GO 4** and **GO 6**.

The proton conductivity was evaluated by electrochemical impedance spectroscopy (EIS). The Nyquist plot of **GO 4** and **GO 6** showed three types of resistance, R, R_1, and R_2 (Fig. 4a and 4b). The proton conductivity was calculated from the R values given by the electrical circuit (Fig. S9) and considering the pellet thickness and surface area. The R value for **GO 4** was 7.0 Ohm (inset in Fig. 4a), while the R value for **GO 6** was 509.4 Ohm (inset in Fig. 4b). The proton conductivity of **GO 4** and **GO 6** was 7×10^{-3} S cm^{-1} and 6×10^{-5} S cm^{-1}, respectively. These results indicate that **GO 4** has a higher proton conductivity, which may be due to the fast ion transportation facilitated by the presence of sulfonic acid functional groups [45]. The proton

conductivity of **GO 3** was also measured. The R value of **GO 3** was 11.0 Ohm (Fig. S10). The proton conductivity of **GO 3** was lower (4×10^{-3} S cm^{-1}) than **GO 4**. This behavior is likely due to the fact that the redox-active functional groups (e.g., 1,4-benzoquinone, hydroquinone) can support the ion transformation, which locates vicinal to proton conductive moieties.

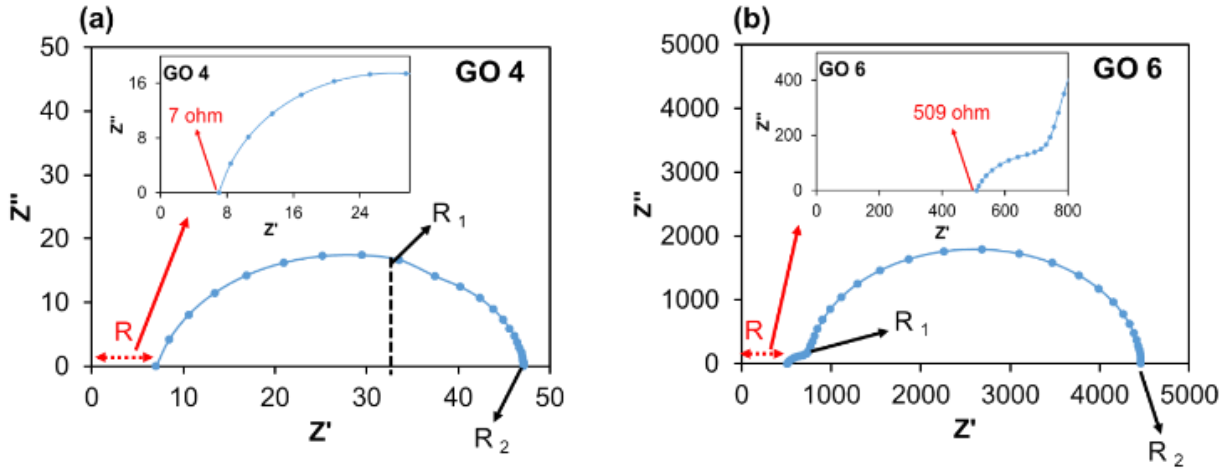

Fig. 4. Impedance spectra of (a) **GO 4** and (b) **GO 6**.

3.3. Double functionalization of GO for enhanced capacitance

To show additional advantages of double functionalized GO, we introduced two similar functions onto GO to increase the performance for supercapacitors. Functionalized carbon materials with redox-active molecules have been applied for sensors [46], supercapacitors [47], and batteries [48]. Here, we introduced 2-amino naphthoquinone and benzoquinone onto GO (**GO 8**) using the stepwise covalent double functionalization method (Fig. 5a). For comparison, mono functionalized GO with 2-amino naphthoquinone (**GO 7**) and benzoquinone (**GO 9**) were prepared (Fig. 5b). The prepared materials (**GO 7**, **GO 8**, and **GO 9**) were confirmed by XPS analysis (see details of the characterization in Section 3 of the Supporting Information).
The electrochemical behavior of **GO 8** was evaluated by CV measurements, comparing those of **GO 7** and **GO 9**. **GO 8** showed oxidation peaks at 0.17 V and 0.54 V, and reduction peaks at 0.10 V and 0.50 V (Fig. 6a-ii), respectively. Similar peaks were observed for mono-functionalized **GO 7** (oxidation peak at 0.15 V and a reduction peak at 0.12 V) (Fig. 6a-i) and **GO 9** (oxidation peak at 0.53 V and a reduction peak at 0.51 V) (Fig. 6a-iii). These results suggest a successful functionalization of GO with two different quinone-based molecules.

Furthermore, the CV curves suggest that **GO 8** has higher capacitance than **GO 7** and **GO 9**. This enhanced capacitance is due to the introduction of more quinone molecules, confirming the advantage of the covalent double functionalization. When the CV curves of **GO 8** were acquired using different scan rates, all the curves maintained their shape, indicating a stable capacitive behavior of this conjugate (Fig. S15). The electrochemical performance of **GO 8** was also compared with **GO 2b** (GO functionalized by a simple amine, followed by the attachment of benzoquinone). The CV curve of **GO 7** demonstrated higher electrochemical performance than **GO 2b** (Fig. S16). Next, the rate capabilities of **GO 7**, **GO 8**, and **GO 9** were measured at different current densities (1 A g^{-1}, 3 A g^{-1}, 5 A g^{-1}, 10 A g^{-1}, 20 A g^{-1}, and 30 A g^{-1}). The specific capacitance of **GO 7**, **GO 8**, and **GO 9** was 100 F g^{-1}, 254 F g^{-1}, and 154 F g^{-1}, respectively, at a current density of 1 A g^{-1} (Fig. 6b). **GO 8** showed higher specific capacitance than **GO 7** and **GO 9**, due to the introduction of more redox-active functionalities onto GO surface. Fig. S18a shows that the galvanostatic charge/discharge curves of **GO 7**, **GO 8**, and **GO 9**. **GO 8** was endowed of a stable capacitance in comparison to **GO 7** and **GO 9**. The nonlinear charge/discharge curves indicate a pseudocapacitive behavior of **GO 8**. These results suggest that stepwise covalent double functionalization successfully introduced more functionalities onto GO and enhanced the supercapacitor performance.

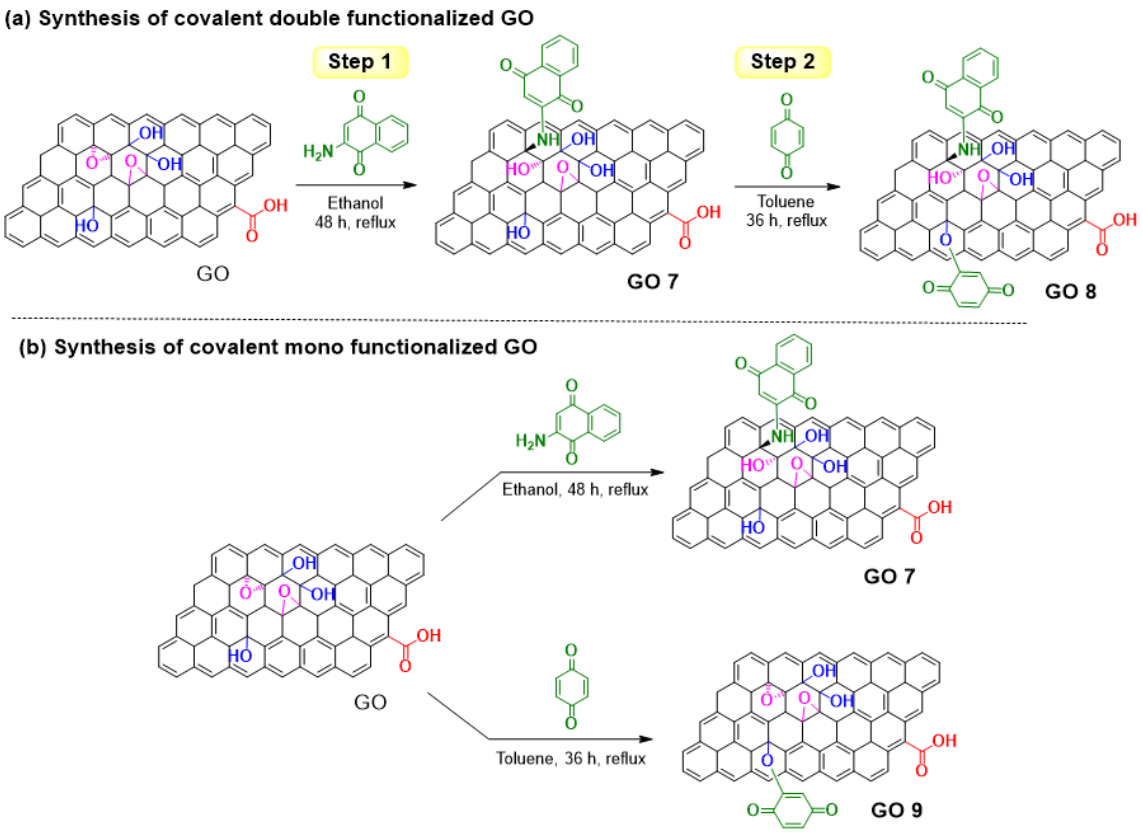

Fig. 5. Synthesis of (a) doubly functionalized **GO 8**; (b) mono functionalized **GO 7** and **GO 9**. For simplicity, only one epoxide ring is opened and one hydroxyl group is derivatized in GO.

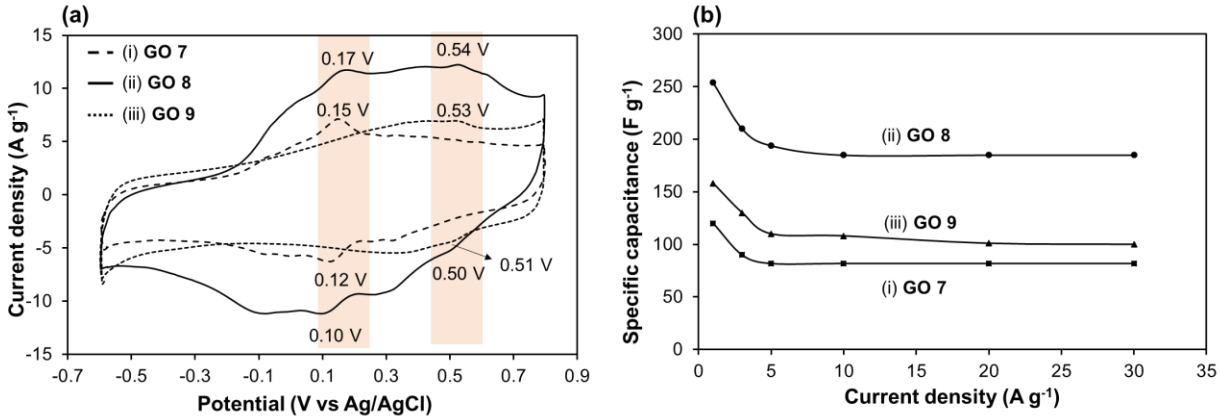

Fig. 6. (a) CV profile of (i) **GO 7**, (ii) **GO 8**, and (iii) **GO 9**, at a scan rate of 50 mV s^{-1}; (b) specific capacitance of (i) **GO 7**, (ii) **GO 8**, and (iii) **GO 9** as a function of current density.

4. Conclusions

In this study, we introduced a series of organic molecules onto the surface of GO by using a stepwise covalent double functionalization. In the first step, the aminated compounds were

reacted with the epoxide groups onto the basal plane of GO. The mono-functionalized GO, containing more OH groups than pristine GO, was then conjugated with α,β-unsaturated carbonyl compounds. This strategy has two advantages: 1) two different functions, and 2) more functions can be introduced. In this paper, we also explored the possibility of endowing GO with acidic and redox properties, aiming at the development of proton conductive electrode materials. As a result, high proton conductivity was obtained using a single material **GO 4**. Furthermore, redox-active quinone molecules were twice introduced, aiming at the synthesis of high capacitance electrodes. The improved capacitance was observed by doubly introducing quinone molecules to GO (**GO 8**). Overall, this research evidence that the double functionalization strategy is effective in preparing multifunctional materials for different applications.

Acknowledgements

This research was supported by JSPS KAKENHI (19H02718) and JST CREST (JPMJCR18R3). We also acknowledge the Centre National de la Recherche Scientifique (CNRS) through the international research project "MULTIDIM" between I2CT Unit and Okayama University.

References

[1] D. Chen, H. Feng, J. Li, *Chem. Rev.* 112 (2012), 6027-6053, https://doi.org/10.1021/cr300115g.

[2] R. K. Singh, R. Kumar, D. P. Singh, *RSC Adv.* 6 (2016), 64993-65011, https://doi.org/10.1039/C6RA07626B.

[3] B. Zhan, C. Li, J. Yang, G. Jenkins, W. Huang, X. Dong, *Small* 10 (2014), 4042-4065, https://doi.org/10.1002/smll.201400463.

[4] Pang, Y. Hernandez, X. Feng, K. Müllen, *Adv. Mater.* 23 (2011), 2779-2795, https://doi.org/10.1002/adma.201100304.

[5] H. Huang, S. Su, N. Wu, H. Wan, S. Wan, H. Bi, L. Sun, *Front Chem.*7 (2019), 399, https://doi.org/10.3389/fchem.2019.00399.

[6] W. Yuan, G. Shi, *J. Mater. Chem. A*, 1 (2013), 10078-10091, https://doi.org/10.1039/C3TA11774J.

[7] M. Hernaez, *Sensors*, 20 (2020). https://doi.org/10.3390/s20113196.

[8] T. Kuilla, S. Bhadra, D. Yao, N. H. Kim, S. Bose, J. H. Lee, *Prog. Polym. Sci.* (2010), 1350-1375, https://doi.org/10.1016/j.progpolymsci.2010.07.005.

[9] C. Wang, Y. Yang, R. Li, D. Wu, Y. Qin, Y. Kong, *Chem. Commun.* 56 (2020), 4003-4006, https://doi.org/10.1039/D0CC01028F.

[10] D. Majumdar, *Innov. Energy Res.* 5 (2016), 1-9.

[11] Z. Xu, H. Sun, X. Zhao, C. Gao, *Adv. Mater.* 25 (2013), 188-193, https://doi.org/10.1002/adma.201203448.

[12] V. Mazánek, J. Luxa, S. Matějková, J. Kučera, D. Sedmidubský, M. Pumera, Z. Sofer, *ACS Nano* 13 (2019), 1574-1582, https://doi.org/10.1021/acsnano.8b07534.

[13] D. Higgins, P. Zamani, A. Yu, Z. Chen, *Energy Environ. Sci.* 9 (2016), 357-390, https://doi.org/10.1039/C5EE02474A.

[14] D. Geng, N. Ding, T. S. A. Hor, Z. Liu, X. Sun, Y. Zong, *J. Mater. Chem. A* 3 (2015), 1795-1810, https://doi.org/10.1039/C4TA06008C.

[15] R. Khan, R. Nakagawa, B. Campeon, Y. Nishina, *ACS Appl. Mater. Interf.* 12 (2020), 12736-12742, https://doi.org/10.1021/acsami.9b21082.

[16] J, Zhu.; D, Yang, Z, Yen, Q, Yan, H, Zhang. *Small* 10 (2014), 3480-3498, https://doi.org/10.1002/smll.201303202.

[17] V. Georgakilas, M. Otyepka, A. B. Bourlinos, V. Chandra, N. Kim, K. C. Kemp, P. Hobza, R. Zboril, K. S. Kim, *Chem. Rev.* 112 (2012), 6156, https://doi.org/10.1021/cr3000412.

[18] M. Cano, U. Khan, T. Sainsbury, A. O'Neill, Z. Wang, I. T. McGovern, W. K. Maser, A. M. Benito, J. N. Coleman, *Carbon* 52 (2013), 363-371, https://doi.org/10.1016/j.carbon.2012.09.046.

[19] S. Stankovich, R. D. Piner, S. T. Nguyen, R. S. Ruoff, *Carbon* 44 (2006), 3342-3347, https://doi.org/10.1016/j.carbon.2006.06.004.

[20] I. A. Vacchi, J. Raya, A. Bianco, C. Ménard-Moyon, *2D Mater.* 5 (2018), 035037, https://doi.org/10.1088/2053-1583/aac8a9.

[21] P. Ji, W. Zhang, S. Ai, Y. Zhang, J. Liu, J. Liu, P. He, Y. Li, *Nanotechnol.* 30 (2019), 115701, https://doi.org/10.1088/1361-6528/aaf8e4.

[22] S. A. Sydlik, T. M. Swager, *Adv. Funct. Mater.* 23 (2013), 1873-1882, https://doi.org/10.1002/adfm.201201954.

[23] I. A. Vacchi, C. Spinato, J. Raya, A. Bianco, C. Ménard-Moyon, *Nanoscale* 8 (2016), 13714-13721, https://doi.org/10.1039/C6NR03846H.

[24] B. Xue, J. Zhu, N. Liu, Y. Li, *Catal. Commun.* 64 (2015), 105-109, https://doi.org/10.1016/j.catcom.2015.02.003.

[25] I. A. Vacchi, S. Guo, J. Raya, A. Bianco, C. Ménard-Moyon, *Chem. Eur. J.* 26 (2020), 6591, https://doi.org/10.1002/chem.201905785.

[26] J. Park, M. Yan, *Acc. Chem. Res.* 46 (2013), 181-189, https://doi.org/10.1021/ar300172h.

[27] S. Guo, Y. Nishina, A. Bianco, C. Ménard-Moyon, *Angew. Chem. Int. Ed.* 132 (2020), 1558-1563, https://doi.org/10.1002/ange.201913461.

[28] E. S. Inks, B. J. Josey, S. R. Jesinkey, C. J. Chou, *ACS Chem. Biol*. 7 (2012), 331, 10.1021/cb200134p.

[29] R. Khan, Y. Nishina, *J. Mater. Chem. A* 8 (2020), 13718, https://doi.org/10.1039/D0TA05489E.

[30] T. Ando, S. Yubuchi, A. Sakuda, A. Hayashi, M. Tatsumisago, *Electrochem.* 87 (2019), 289, https://doi.org/10.1016/j.elecom.2020.106741.

[31] J. Yan, G. Chen, J. Cao, W. Yang, B. Xie, M. Yang, *New Carbon Mater.* 27 (2012), 370, https://doi.org/10.1016/S1872-5805(12)60022-5.

[32] F. Zhou, H. N. Tien, Q. Dong, W. L. Xu, H. Li, S. Li, M. Yu, *J. Membrane Sci.* 573 (2019), 184-191, https://doi.org/10.1016/j.memsci.2018.11.080.

[33] F. Samadaei, M. Salami-Kalajahi, H. Roghani-Mamaqani, M. Banaei, *RSC Adv.* 5 (2015), 71835-71843, https://doi.org/10.1039/C5RA12086A.

[34] Y. Ding, F. Zhang, J. Xu, Y. Miao, Y. Yang, X. Liu, B. Xu, *RSC Adv.* 7 (2017), 28754-28762, https://doi.org/10.1039/C7RA02421E.

[35] Z. Liu, L. Wang, G. Ma, Y. Yuan, H. Jia, W. Fei, *J. Mater. Chem. A* 8 (2020), 18933-18944, https://doi.org/10.1039/D0TA06042A.

[36] X. Wang, J. Wu, L. Zhou, X. Wei, W. Wang, *Proc. Inst. of Mech. Eng.* 232 (2018), 1428-1436, https://doi.org/10.1177/1350650117754000.

[37] F. Zhou, H. N. Tien, Q. Dong, W. L. Xu, H. Li, S. Li, M. Yu, *J. Membr. Sci.* 573 (2019), 184, https://doi.org/10.1016/j.memsci.2018.11.080.

[38] L. Chen, Z. Xu, J. Li, B. Zhou, M. Shan, Y. Li, L. Liu, B. Li, J. Niu, *RSC Adv.* 4 (2014), 1025-1041, https://doi.org/10.1039/C3RA46203J.

[39] F. Han, S. Yang, W. Jing, K. Jiang, Z. Jiang, H. Liu, L. Li, *Opt. Express* 22 (2014), 11436-11445, https://doi.org/10.1364/OE.22.011436.

[40] Q. Chen, J. Sun, P. Li, I. Hod, P. Z. Moghadam, Z. S. Kean, R. Q. Snurr, J. T. Hupp, O. K. Farha, J. F. Stoddart, *J. Am. Chem. Soc.* 138 (2016), 14242-14245, 10.1021/jacs.6b09880.

[41] L. Hou, Z. Hu, H. Wu, X. Wang, Y. Xie, S. Li, F. Ma, C. Zhu, *Dalton Trans.* 48 (2019), 9234-9242, https://doi.org/10.1039/C9DT00895K.

[42] M. Boota, C. Chen, M. Bécuwe, L. Miao, Y. Gogotsi, *Energy Environ. Sci.* 9 (2016), 2586-2594, https://doi.org/10.1039/C6EE00793G.

[43] J. Wang, A. E. Lakraychi, X. Liu, L. Sieuw, C. Morari, P. Poizot, A. Vlad, *Nat. Mater.* 1 (2020), https://doi.org/10.1038/s41563-020-00869-1.

[44] C. Yin, J. Li, Y. Zhou, H. Zhang, P. Fang, C. He, *ACS Appl. Mater. Interf.* 10 (2018), 14026-14035, https://doi.org/10.1021/acsami.8b01513.

[45] A. Khabibullin, S. D. Minteer, I. Zharov, *J. Mater. Chem. A* 2 (2014), 12761-12769, https://doi.org/10.1039/C4TA01202J.

[46] N. Ashwin Karthick, R. Thangappan, M. Arivanandhan, A. Gnanamani, R. Jayavel, *J. Inorg. Organomet. Polym.* 28 (2018), 1021, https://doi.org/10.1007/s10904-017-0744-0.

[47] R. Khan, Y. Nishina, *Nanoscale* 13 (2021), 36-50, https://doi.org/10.1039/D0NR07500K.

[48] Y. Li, Z. Jian, M. Lang, C. Zhang, X. Huang, *ACS Appl. Mater. Interf.* 8 (2016), 1735, https://doi.org/10.1021/acsami.6b05271.